

Hydrogen Atom Transfer Reactions of the Unsaturated Hydroxycarbonyne Complex $[W_2Cp_2(\mu-COH)(\mu-PPh_2)_2]BF_4$

Fernanda Cimadevilla,[†] M. Esther García,[†] Daniel García-Vivó,[†] Miguel A. Ruiz,^{*,†} Claudia Graiff,[‡] and Antonio Tiripicchio[‡]

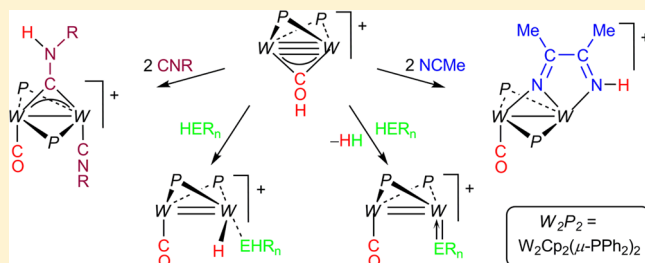
[†]Departamento de Química Orgánica e Inorgánica/IUQOEM, Universidad de Oviedo, E-33071 Oviedo, Spain

[‡]Dipartimento di Chimica, Università di Parma, Viale delle Scienze 17/A, I-43100 Parma, Italy

S Supporting Information

ABSTRACT: The hydroxycarbonyne complex salt $[W_2Cp_2(\mu-COH)(\mu-PPh_2)_2]BF_4$ (**1**) reacted rapidly with water in the presence of the oxidant $[FeCp_2]BF_4$ to give the hydroxo complex salt $[W_2Cp_2(OH)(\mu-PPh_2)_2(CO)]BF_4$, a preparation that could be replicated using the neutral carbonyl complex $[W_2Cp_2(\mu-PPh_2)_2(\mu-CO)]$ (**2**) instead. A similar reaction took place slowly with HSPH and rapidly in the presence of $[FeCp_2]BF_4$, to yield the known 32-electron complex salt $[W_2Cp_2(SPh)(\mu-PPh_2)_2(CO)]BF_4$. In contrast, **1** did not react with PhOH or H_2Np -tol even in the presence of $[FeCp_2]BF_4$.

However, a fast reaction between these molecules and **2** took place in the presence of $[FeCp_2]BF_4$, to give the phenolato complex salt $[W_2Cp_2(OPh)(\mu-PPh_2)_2(CO)]BF_4$ and the imido-hydride $[W_2Cp_2(\mu-H)(Np$ -tol) $(\mu-PPh_2)_2(CO)]BF_4$ ($W-W = 2.9135(8)$ Å), respectively, after formal elimination of hydrogen. The hydroxycarbonyne complex **1** reacted rapidly with PH_2Cy to give the hydride derivative $[W_2Cp_2(H)(\mu-PPh_2)_2(CO)(PH_2Cy)]BF_4$, this requiring H-migration from O to W atoms. The M–H bonds in the latter hydride cations were deprotonated by strong bases to give the corresponding neutral complexes $[W_2Cp_2(Np$ -tol) $(\mu-PPh_2)_2(CO)]$ and $[W_2Cp_2(\mu-PPh_2)_2(CO)(PH_2Cy)]$. Compound **1** also reacted easily with two-electron donors such as NCMe, CN^tBu , and CNp -tol, to give products derived from the addition of two molecules of reagent in each case, and some rearrangement of the COH ligand. The first reaction gave the new cationic complex $[W_2Cp_2(\mu-PPh_2)_2(\mu-N:N,N'-N_2HC_2Me_2)(CO)]BF_4$, derived from the C–C coupling of two nitrile molecules accompanied by an O to N shift of the hydroxycarbonyne proton. In contrast, no C–C coupling processes were observed in the reactions with isocyanides, although proton migration occurred in all cases, either to the metal (reaction with CN^tBu), to give the hydride $[W_2Cp_2(H)(\mu-PPh_2)_2(\mu-CN^tBu)(CN^tBu)]BF_4$, or to the N atom of one of the incoming isocyanides (reaction with CNp -tol), to give the aminocarbonyne derivative $[W_2Cp_2\{\mu-CN(H)p$ -tol $\}(\mu-PPh_2)_2(CNp$ -tol) $(CO)]BF_4$.



INTRODUCTION

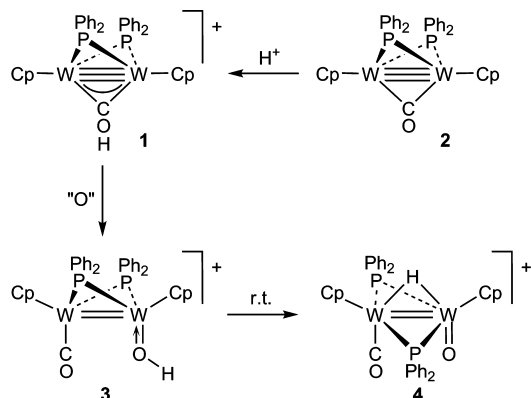
Some time ago we reported the preparation of the cationic hydroxycarbonyne complex salt $[W_2Cp_2(\mu-COH)(\mu-PPh_2)_2]BF_4$ (**1**), a species selectively formed via O-protonation of the bridging carbonyl in the neutral complex $[W_2Cp_2(\mu-PPh_2)_2(\mu-CO)]$ (**2**) (Scheme 1).¹ At that time, **1** was the first reported complex having a hydroxycarbonyne ligand bridging a triple metal–metal bond and the second hydroxycarbonyne complex with enough thermal stability so as to be handled at room temperature.² Not unexpectedly, the combined presence of multiple M–M and M–C bonds in this cation makes it quite reactive; actually, this species was found to be quite air-sensitive, transforming progressively into the hydroxo carbonyl derivative $[W_2Cp_2(OH)(\mu-PPh_2)_2(CO)]BF_4$ (**3**), which in turn underwent an unusual intramolecular oxidative addition of the O–H bond at room temperature, to give the oxohydride isomer $[W_2Cp_2(\mu-H)(O)(\mu-PPh_2)_2(CO)]BF_4$ (**4**) (Scheme 1).¹ The formation of **3** apparently followed from the reaction of **1** with oxygen, but no proof of it was obtained at the time.

The above studies were followed by a systematic study on the synthesis and reactivity of related methoxycarbonyne-bridged species. We could thus easily prepare the 30-electron complexes $[W_2Cp_2(\mu-COMe)(\mu-PPh_2)_2]CF_3SO_3$,¹ $[M_2Cp_2(\mu-COMe)(\mu-PCy_2)(\mu-CO)]$ ($M = Mo^{3a,b}, W$),^{3c} $[Mo_2Cp_2(\mu-COMe)_2(\mu-PCy_2)]BF_4$,⁴ $[Mo_2Cp_2(\mu-COMe)(\mu-PET_2)]BF_4$,^{4a} and $[Mo_2Cp_2(\mu-COMe)(\mu-CPh)(\mu-PCy_2)]CF_3SO_3$ by O-methylation of suitable carbonyl-bridged precursors. These methoxycarbonyne complexes were found to be more robust than their hydroxycarbonyne analogues but still retained a high reactivity derived from the unusual combination of multiple M–M and M–C bonds. The reactivity of the cationic complexes was dominated by the electrophilic nature of the unsaturated dimetal center.^{1,2,4b,5,6} In contrast, the neutral complex $[Mo_2Cp_2(\mu-COMe)(\mu-PCy_2)(\mu-CO)]$ had a biphilic behavior, actually displaying a remarkable multisite reactivity involving not only the multiple Mo–Mo and Mo–C bonds but also the

Received: June 21, 2013



Scheme 1



essentially single C–O and O–Me bonds of the methoxycarbonyl ligand.⁷ In the course of all these studies we also prepared some dimolybdenum hydroxycarbonyl complex salts related to the ditungsten complex **1**, such as $[\text{Mo}_2\text{Cp}_2(\mu\text{-COH})(\mu\text{-PCy}_2)_2]\text{BF}_4$,⁸ $[\text{Mo}_2\text{Cp}_2(\mu\text{-COH})(\mu\text{-PEt}_2)_2]\text{BF}_4$,^{4a} and $[\text{Mo}_2\text{Cp}_2(\mu\text{-COH})(\mu\text{-COMe})(\mu\text{-PCy}_2)]\text{BF}_4$.^{4a} However, only the former proved to be stable enough at room temperature (although decomposing in solution slowly), while the latter two compounds evolved at room temperature to give hydride-carbonyl isomers, which in turn were also unstable species decomposing progressively upon manipulation.

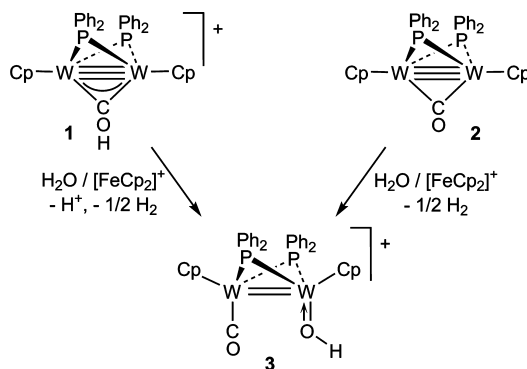
In summary, the chemical behavior of hydroxycarbonyl complexes remains largely unexplored to date. Yet, any study of the reactivity of the hydroxycarbonyl ligand at an unsaturated dimetal center might be of interest not only because of the unusual transformations that can be induced by the coexistence of different multiple bonds (M–M and M–C) in the same substrate, but also in the context of the metal-catalyzed hydrogenation processes of carbon monoxide.⁹ In fact, we have observed some relevant transformations related to the Fischer–Tropsch synthesis in our previous work on the 32-electron hydroxycarbonyl complex $[\text{W}_2\text{Cp}_2(\mu\text{-COH})(\mu\text{-Ph}_2\text{PCH}_2\text{PPh}_2)(\text{CO})_2]^+$, including an unusual reduction to CH_4 ,^{2c} and the insertion of CH_2 into the O–H bond or its coupling with the carbonyl ligand.^{2a} It was thus of interest to examine the chemical behavior of even more unsaturated hydroxycarbonyl complexes such as the 30-electron cation of compound **1**, which is the purpose of the present paper. We have now revisited its unusual transformation into the hydroxo species **3** and analyzed its reactivity toward simple donors such as isocyanides and nitriles and donors having potentially reactive E–H bonds (E = O, S, N, P). We have found that the latter reactions can be greatly accelerated in the presence of the oxidant $[\text{FeCp}_2]\text{BF}_4$, in a process that can be essentially replicated using the neutral complex **2** and involves the highly reactive radical cation $[\text{W}_2\text{Cp}_2(\mu\text{-PPh}_2)_2(\mu\text{-CO})]^+$. We note that we have recently used a similar strategy to increase the reactivity of the isoelectronic and isostructural benzylidyne complex $[\text{Mo}_2\text{Cp}_2(\mu\text{-CPh})(\mu\text{-PCy}_2)(\mu\text{-CO})]$.¹⁰ As it will be shown below, all reactions of **1** involve the cleavage of the O–H bond of the hydroxycarbonyl ligand by following at least four different pathways: (a) dehydrogenation in the reactions with E–H molecules, (b) deprotonation following oxidation, (c) H-transfer to the metal center, to give hydride derivatives, and (d) H-transfer to the incoming ligand.

RESULTS AND DISCUSSION

Revisiting the Transformation of Compound 1 into 3.

As noted above, compound **1** progressively transforms into the oxohydride **4** via the thermally unstable hydroxo isomer **3**, in a reaction usually requiring a few days for completion in solution (Scheme 1). In our preliminary communication we attributed such transformation to a slow reaction with adventitious oxygen. However, we have now identified water as the actual source of oxygen in this reaction. First, a separate experiment revealed that bubbling dry air through a dichloromethane solution of compound **1** at temperatures in the range 253–273 K (conditions in which the transformation $3 \rightarrow 4$ is very slow) did not speed up the formation of **3** to a significant extent. Second, separate experiments revealed that compound **1** also failed to react with other potential sources of oxygen, such as olefin oxides. In contrast, the transformation of **1** into the oxohydride **4** could be completed within a few hours upon addition of water at room temperature to dichloromethane solutions of **1**, in a reaction occurring via the hydroxo isomer **3**, as revealed by IR and $^{31}\text{P}\{^1\text{H}\}$ NMR monitoring. Finally and interestingly, the reaction of **1** with water turned out to be instantaneous in the presence of stoichiometric amounts of the oxidant $[\text{FeCp}_2]\text{BF}_4$, to give **3** (Scheme 2). In the latter case,

Scheme 2



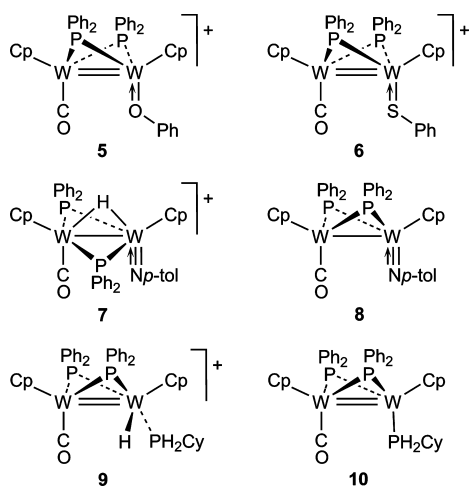
the formation of **3** must be preceded by an oxidized form of the hydroxycarbonyl complex, possibly the (undetected) radical dication $[\text{W}_2\text{Cp}_2(\mu\text{-COH})(\mu\text{-PPh}_2)_2]^{2+}$ (**1**⁺), which would react with a water molecule with overall abstraction of an oxygen atom and release of a proton and an H atom (likely as H_2). Then, we reasoned that 1-electron oxidation in the neutral compound **2** would generate a related radical $[\text{W}_2\text{Cp}_2(\mu\text{-CO})(\mu\text{-PPh}_2)_2]^+$ (**2**⁺), possibly reacting rapidly with water to give **3**, in a reaction paralleling the recently reported redox-induced reactions of the benzylidyne complex $[\text{Mo}_2\text{Cp}_2(\mu\text{-CPh})(\mu\text{-PCy}_2)(\mu\text{-CO})]$.¹⁰ Indeed we found that **2** is rapidly transformed into **3** upon addition of water and $[\text{FeCp}_2]\text{BF}_4$ to dichloromethane solutions of the complex (Scheme 2). The mechanistic aspects of the above transformations will be discussed later on.

Reactions of Compound 1 with HER_n Molecules. We have examined the reactions of **1** with simple donors having E–H bonds common in many biologically relevant molecules (O–H, S–H, and N–H) and a few other ones. However, we have found that these reactions are severely limited by the kinetics, for if the reaction of **1** with the incoming molecule is slow, then reaction with adventitious water occurs preferentially to eventually give the oxohydride **4**. As it will be discussed

below, the redox-induced reactions of **1** or **2** can be used as an alternative strategy, but neither are of general applicability.

Compound **1** does not react at room temperature with phenol even when a large excess of reagent is used: only a slow transformation into the oxohydride **4** was observed, resulting from the reaction with adventitious water, and the same results (but much faster) were obtained in the presence of $[\text{FeCp}_2]\text{BF}_4$. In contrast, the reaction of **2** with phenol in the presence of the latter oxidant rapidly gave the new phenolato complex salt $[\text{W}_2\text{Cp}_2(\text{OPh})(\mu\text{-PPh}_2)_2(\text{CO})]\text{BF}_4$ (**5**) (Chart 1), along

Chart 1



with small amounts of **4** as a side product. Compound **5** is structurally related to the hydroxo complex **3** and also is rather unstable, experiencing progressive hydrolysis upon manipulation, to eventually yield the oxohydride **4**.

Compound **1** reacts slowly with benzenethiol at room temperature, to give the thiolato complex salt $[\text{W}_2\text{Cp}_2(\text{SPh})(\mu\text{-PPh}_2)_2(\text{CO})]\text{BF}_4$ (**6**) (Chart 1), a compound prepared previously in our laboratory from the reaction of **3** with the same reagent.¹¹ Under these conditions, the oxohydride **4** is also formed in variable amounts due to the unavoidable presence of trace amounts of water. Fortunately, this undesired side reaction could be almost completely suppressed in the presence of $[\text{FeCp}_2]\text{BF}_4$, which dramatically increased the rate of reaction of **1** with PhSH . Not surprisingly, compound **6** could be also obtained by reacting **2** with stoichiometric amounts of HSPh in the presence of $[\text{FeCp}_2]\text{BF}_4$, in a process that is both faster and more selective than the one starting from **1**.

Compound **1** does not react with *p*-toluidine, nor does it in the presence of $[\text{FeCp}_2]\text{BF}_4$, the only product formed being the ubiquitous oxohydride **4**. In contrast, compound **2** reacts rapidly with *p*-toluidine in the presence of the same oxidant to give the imido-hydride derivative $[\text{W}_2\text{Cp}_2(\mu\text{-H})(\mu\text{-PPh}_2)_2(\text{CO})]\text{BF}_4$ (**7**) in good yield (Chart 1). Compound **7** is structurally related to the oxohydride **4** and to the sulfido-hydride $[\text{W}_2\text{Cp}_2(\mu\text{-H})(\text{S})(\mu\text{-PPh}_2)_2(\text{CO})]\text{BF}_4$ ¹¹ and can be analogously deprotonated to give a neutral derivative. Indeed, the addition of the strong base 1,8-diazabicycloundec-7-ene (DBU) to dichloromethane solutions of **7** gives the imido complex $[\text{W}_2\text{Cp}_2(\text{Np-tol})(\mu\text{-PPh}_2)_2(\text{CO})]$ (**8**) quantitatively (Chart 1).

We finally examined the reactivity of the hydroxycarbene **1** toward several molecules having P–H bonds. Although no

reaction was observed with secondary phosphines, a slow reaction took place with cyclohexylphosphine at room temperature to give the hydride derivative $[\text{W}_2\text{Cp}_2(\text{H})(\mu\text{-PPh}_2)_2(\text{CO})(\text{PH}_2\text{Cy})]\text{BF}_4$ (**9**), which displays a coordinated molecule of phosphine (Chart 1). As with the case of **7**, the hydride ligand in **9** can be easily removed through deprotonation with DBU, to give the neutral phosphine complex $[\text{W}_2\text{Cp}_2(\mu\text{-PPh}_2)_2(\text{CO})(\text{PH}_2\text{Cy})]$ (**10**) in high yield (Chart 1).

Structural Characterization of Compound 5. The spectroscopic data available for the phenolato complex **5** are similar to those of the related hydroxo (**3**) and thiolato (**6**) complexes (Table 1). Therefore, a similar structure is to be

Table 1. Selected IR and $^{31}\text{P}\{^1\text{H}\}$ NMR Data for New Compounds

compound	$\nu(\text{CO})^a$	$\delta_{\text{P}} (J_{\text{PP}})^b$	J_{PW}^c
$[\text{W}_2\text{Cp}_2(\mu\text{-COH})(\mu\text{-PPh}_2)_2]\text{BF}_4$ (1) ^d		186.8	364
$[\text{W}_2\text{Cp}_2(\text{OPh})(\mu\text{-PPh}_2)_2(\text{CO})]\text{BF}_4$ (5)	1914 (s)	117.7	381, 272
$[\text{W}_2\text{Cp}_2(\text{SPh})(\mu\text{-PPh}_2)_2(\text{CO})]\text{BF}_4$ (6) ^e	1926 (s)	111.7	370, 266
$[\text{W}_2\text{Cp}_2(\mu\text{-H})(\text{Np-tol})(\mu\text{-PPh}_2)_2(\text{CO})]\text{BF}_4$ (7)	1959 (s)	40.8	267, 248
$[\text{W}_2\text{Cp}_2(\text{Np-tol})(\mu\text{-PPh}_2)_2(\text{CO})]$ (8)	1833 (s)	109.2	385, 304
$[\text{W}_2\text{Cp}_2(\text{H})(\mu\text{-PPh}_2)_2(\text{CO})(\text{PH}_2\text{Cy})]\text{BF}_4$ (9)	1895 (s)	115.2 100.6 (20) −25.5 (20)	278, 188 367, 206 207
$[\text{W}_2\text{Cp}_2(\mu\text{-PPh}_2)_2(\text{CO})(\text{PH}_2\text{Cy})]$ (10)	1855 (s)	81.7 −14.9	334, 334 395
$[\text{W}_2\text{Cp}_2(\mu\text{-PPh}_2)_2(\mu\text{-N:N,N',N'}\text{-N}_2\text{HC}_2\text{Me}_2)(\text{CO})]\text{BF}_4$ (11)	1912 (s)	−25.1	251, 235
$[\text{W}_2\text{Cp}_2(\text{H})(\mu\text{-PPh}_2)_2(\mu\text{-CN}^t\text{Bu})(\text{CN}^t\text{Bu})]\text{BF}_4$ (12)	2140 (vs) ^f 1950 (s) ^f	60.5	319, 245
$[\text{W}_2\text{Cp}_2\{\mu\text{-CN}(\text{H})p\text{-tol}\}(\mu\text{-PPh}_2)_2(\text{CN}p\text{-tol})(\text{CO})]\text{BF}_4$ (13)	2108 (vs) ^f 1960 (s)	−24.3 ^g −26.2 ^h	229, 224 ^g 229, 222 ^h

^aRecorded in CH_2Cl_2 solution unless otherwise stated, with C–O stretching frequencies in cm^{-1} . ^bRecorded at room temperature in CD_2Cl_2 solutions unless otherwise stated; δ in ppm relative to external 85% aqueous H_3PO_4 , with coupling to phosphorus indicated in brackets (J_{PP} in Hz). ^cOne-bond ^{31}P – ^{183}W coupling constants in Hz. ^dData taken from ref 1. ^eData taken from ref 11. ^fValues corresponding to the C–N stretching frequencies. ^gValues for isomer **13a**. ^hValues for isomer **13b**.

assumed for this molecule, with a cisoid arrangement of the Cp ligands, as determined crystallographically for **6**.¹¹ Of particular relevance in this respect are the values of the C–O stretching frequencies in these compounds [1908 (**3**) < 1914 (**5**) < 1926 (**6**) cm^{-1}], which suggest that the phenolato ligand has a π -donor ability intermediate between those of the hydroxo (stronger donor) and thiolato (weaker donor) ligands. Moreover, **5** displays a single ^{31}P NMR resonance with medium to high one-bond P–W couplings (381 and 272 Hz) comparable to those measured for **3** (372 and 281 Hz) and **6** (370 and 266 Hz),¹¹ in agreement with the similar and relatively low-coordination environments of the metal centers in all of these molecules.¹²

Structural Characterization of the Imido Compounds 7 and 8. The cation in compound **7** (Figure 1 and Table 2) is built from two cisoid WCp fragments bridged by a hydride and two transoid PPh₂ ligands, the latter defining a flat W_2P_2

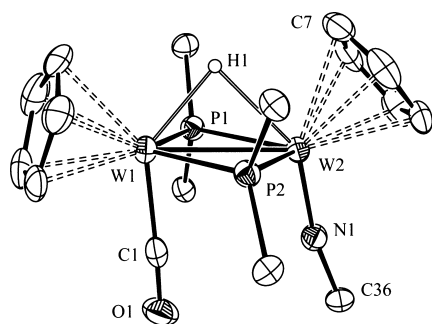


Figure 1. ORTEP diagram (30% probability) of the cation in compound **7** with H atoms (except the hydride ligand) and Ph and *p*-tol groups (except their C¹ atoms) omitted for clarity.

Table 2. Selected Bond Lengths (Å) and Angles (deg) for Compound **7**

W(1)–W(2)	2.9135(8)	W(1)–P(1)–W(2)	73.93(6)
W(1)–P(1)	2.374(2)	W(1)–P(2)–W(2)	73.61(6)
W(1)–P(2)	2.388(2)	C(1)–W(1)–W(2)	80.9(2)
W(2)–P(1)	2.469(2)	C(1)–W(1)–P(1)	85.2(2)
W(2)–P(2)	2.474(2)	C(1)–W(1)–P(2)	84.3(2)
W(1)–C(1)	1.980(10)	N(1)–W(2)–W(1)	104.6(2)
C(1)–O(1)	1.164(10)	N(1)–W(2)–P(1)	99.1(2)
W(2)–N(1)	1.759(8)	N(1)–W(2)–P(2)	98.8(2)
N(1)–C(36)	1.405(10)	W(2)–N(1)–C(36)	167.2(6)
		W(1)–C(1)–O(1)	176.3(7)

rhombus, with the coordination sphere of the metals being completed with either CO or *Np*-tol terminal ligands, almost parallel to each other, with the first one leaning toward the intermetallic center (C–W–W 80.9(2)°) and the second one pointing away from it (N–W–W 104.6(2)°). The W(2)–N(1) length of 1.759(8) Å is consistent with the formulation of a triple bond between these atoms, this value being comparable to those measured in related complexes having W≡N bonds such as [W₂Cp₂(μ-PPh₂)₂(κ¹-N₂CPh₂)(CO)]^{6a}, [W₂Cp₂{NC(CMe₂)(Ar)}(μ-CO)(CO)₃], [Mo₂Cp₂*₂{NC(CMe₂)(Ph)}(μ-CO)₂(CO)₂]¹³, [MCp*ClMe₂(N^tBu)] (M = Mo and W),¹⁴ [WTP⁺(CO)₂(NR)] PF₆ (Tp⁺ = hydrottris(3,5-dimethylpyrazolyl)borate; R = Ph, ^tBu),¹⁵ or [W(NCy)Cl(PMe₃)₄]BPh₄,¹⁶ in the range 1.71–1.79 Å. This bond multiplicity is also supported by the almost linear conformation of the W(2)–N(1)–C(36) chain (167.2(6)°), as expected for a sp-hybridized N atom. In fact, the small deviation from linearity observed might be caused by an incipient steric clash between one of the phenyl groups of the PPh₂ ligands and the aromatic ring of the imido group. As observed for the complexes mentioned above, the imido group in **7** exerts a strong labilizing effect. As a result, the P atoms bridge the metal atoms somewhat asymmetrically (Δ*d* ca. 0.1 Å), being closer to the W(CO) fragment, as expected from the different donor ability of the terminal ligands involved (CO vs *Np*-tol). This effect can be also noticed in the W(2)–Cp bonding, with a particularly larger elongation of the bond involving the C atom *trans* to the N atom (W(2)–C(7) = 2.377(10) Å). In all, the NR group would be acting as a four-electron donor, and therefore a single metal–metal bond should be formulated for this cation under the effective atomic number (EAN) formalism. This is consistent with the intermetallic distance of 2.9135(8) Å, which still might be viewed as somewhat short for an electron-precise molecule. However, we^{6a} and others¹⁷ have found

previously that the presence of three monodentate bridging ligands causes a systematic decrease of the intermetallic distances. Indeed, this is the case of the isoelectronic and isostructural complexes [W₂Cp₂(μ-COMe)(μ-PPh₂)₂(CO)₂]-BF₄ (2.9020(5) Å) and [W₂Cp₂(μ-COMe)(μ-PPh₂)₂(μ-dmpm)]BF₄ (2.917(1) Å).^{6a}

The spectroscopic data available in solution for **7** (Table 1 and Experimental Section) are fully consistent with its solid-state structure and indicative of its close structural relationship with the oxohydride **4** and the sulfido hydride [W₂Cp₂(μ-H)(μ-PPh₂)₂(S)(CO)]BF₄.¹¹ For instance, **7** displays a single ³¹P NMR resonance (δ 40.8 ppm, *J*_{PW} = 267, 248 Hz) with chemical shift and P–W couplings comparable to those of **4** (δ 31.3 ppm, *J*_{PW} = 280, 246 Hz)¹ and the sulfido hydride complex (δ 36.8 ppm, *J*_{PW} = 244, 228 Hz).¹¹ Its IR spectrum displays a C–O stretching band (1959 cm^{−1}) significantly less energetic than those in the mentioned complexes (cf. 1977 cm^{−1} for **4**), reflecting the stronger π-donor ability of the imido ligand. Finally, the presence of a bridging hydride ligand in **7** is clearly denoted by the appearance of a strongly shielded resonance at −9.18 ppm in its ¹H NMR spectrum, with chemical shift and P–H and P–W couplings comparable to those reported for **4** and the mentioned sulfido hydride complex.

The spectroscopic data for the neutral imido complex **8** also are comparable to those of the neutral oxo and sulfido complexes [W₂Cp₂(μ-PPh₂)₂(E)(CO)] (E = O,¹ S¹¹); then, a similar structure is to be assumed for this molecule, with a cisoid arrangement of the Cp ligands. Of particular significance in this respect is that the ³¹P chemical shifts and one-bond P–W couplings of all of these complexes are remarkably similar [δ 109.2 ppm, *J*_{PW} = 385, 304 Hz (**8**), δ 102.2 ppm, *J*_{PW} = 381, 322 Hz (E = O)]. Moreover, the values of the P–W couplings in **8** are substantially higher than those in its precursor **7**, in agreement with the reduction of the coordination number at the metal centers operated upon deprotonation.¹² The IR spectrum of **8** displays one C–O stretching band at 1833 cm^{−1}, a figure that again is substantially lower than those measured for the related oxo and sulfido complexes (1858 and 1863 cm^{−1}, respectively), once more denoting the superior π-donor ability of the imido ligand.

We should note that the strong spectroscopic similarities found between the imido complexes **7** and **8** and their cationic and neutral oxo and sulfido counterparts reveals that the π-bonding contribution (ligand to metal) in the latter oxo and sulfido complexes, although lower than the corresponding contribution in the imido complexes, might be greater than initially suspected,^{1,11} this implying that the intermetallic bond order in these chalcogeno complexes might actually be intermediate between one and two (rather than two), a matter that we have discussed previously for the isoelectronic oxo complexes [Mo₂Cp₂(μ-CPh)(μ-PCy₂)(O)(CO)]¹⁰.

Structural Characterization of Compounds **9** and **10**.

The presence of a terminal carbonyl ligand in **9** is clearly evidenced by the appearance in the IR spectrum of a C–O stretching band at 1895 cm^{−1}, with a frequency comparable to those measured for related complexes of the type [M₂Cp₂(κ²-L₂)(μ-PPh₂)₂(CO)]⁺ (L₂ = 3-electron bidentate ligand, M = Mo,¹⁸ W).¹¹ The appearance of three resonances in the ³¹P{¹H} NMR spectrum (Table 1) establish the incorporation of the PH₂Cy ligand, in a way that renders inequivalent PPh₂ groups, thus discarding a structure with a bridging hydride ligand comparable to that of **7**. Full assignment of these resonances could be made by considering the number and

values of the observed P–W, P–H, and P–P couplings; thus, the most shielded signal (–25.5 ppm) was easily assigned to the terminal PH_2Cy ligand, on the basis of its coupling to a single ^{183}W nucleus, two P–H hydrogen atoms ($^1J_{\text{PH}} = 370$ Hz) and a hydride ligand ($^2J_{\text{PH}}$ ca. 70 Hz). In addition, by recalling the general trends established for the absolute values of $^2J_{\text{XY}}$ in complexes of the type $[\text{MCpXYL}_2]^+$,^{12,19} ($J_{\text{cis}} > J_{\text{trans}}$), we can identify the PPh_2 resonance displaying larger P–P coupling (δ 100.6 ppm, $^2J_{\text{PP}} = 20$ Hz) as the one corresponding to the group positioned *cis* to the phosphine ligand. Finally, the presence of a terminal hydride ligand is corroborated by the appearance of a poorly shielded resonance in the ^1H NMR spectrum at –0.79 ppm, coupled to the three P atoms of the cation ($J_{\text{HP}} = 67, 36,$ and 11 Hz). This in turn implies that the coordination numbers of the two metal atoms differ by one unit, which is consistent with the large difference between the P–W couplings of each of the PPh_2 groups (Table 1). It should be stressed that the cation **9** is structurally related to the hydride cations $[\text{W}_2\text{Cp}_2(\text{H})(\mu\text{-PR}_2)_2(\text{CO})_2]^+$ ($\text{R} = \text{Ph}, \text{Et}$) initially formed upon protonation of the neutral dicarbonyls *trans*- $[\text{W}_2\text{Cp}_2(\mu\text{-PR}_2)_2(\text{CO})_2]$. These dicarbonyl cations also display poorly shielded hydride resonances (cf. –0.42 ppm, J_{PP} 19 and 12 Hz when $\text{R} = \text{Ph}$).⁸ There are, however, two fundamental differences between these species and **9**: First, they presumably display a transoid arrangement of the constituting WCp fragments, in contrast to the *cis* arrangement presumed for **9**. Second, they are thermally unstable and rearrange at room temperature to the hydride-bridged isomers $[\text{W}_2\text{Cp}_2(\mu\text{-H})(\mu\text{-PR}_2)_2(\text{CO})_2]^+$, with a *cis* arrangement of the carbonyl ligands (confirmed crystallographically in the PPh_2 derivative), a structure comparable to that of the imido hydride **7**. Interestingly, compound **9** proved to be stable in refluxing dichloromethane solution for 4 h.

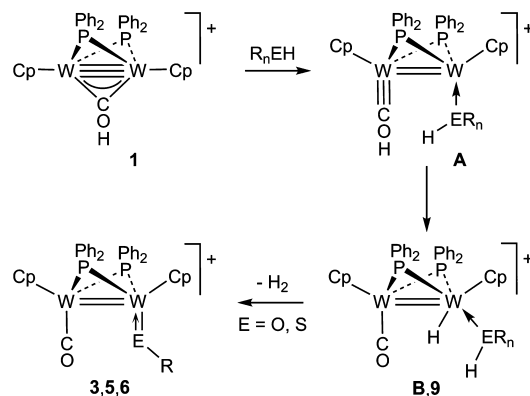
The neutral complex **10** displays a C–O stretching band at 1855 cm^{-1} , a figure some 40 cm^{-1} lower than the corresponding one in its cationic precursor as expected and also lower than the average figure of 1899 cm^{-1} found in the related dicarbonyl complex *cis*- $[\text{W}_2\text{Cp}_2(\mu\text{-PPh}_2)_2(\text{CO})_2]$,⁸ as anticipated for the replacement of a carbonyl group with a poorer acceptor PH_2Cy ligand. The two PPh_2 groups are now equivalent and give rise to a resonance at 81.7 ppm (cf. 74.3 ppm in the mentioned dicarbonyl complex), while the PH_2Cy group gives rise to a relatively shielded signal at 14.9 ppm retaining a large coupling to two protons ($^1J_{\text{PH}} = 340$ Hz). The coordination numbers in this structure are now the same for both W atoms, which is reflected in all P–W couplings having high and comparable values above 300 Hz, in contrast to the dissimilar values observed in the precursor **9** (Table 1).

Pathways in the Reactions of **1** with HER_n Molecules.

As we have discussed above, compound **1** reacts with H_2O , HSPh , and PH_2Cy in the absence of oxidant to yield, in all cases, products in which the hydrogen atom of the hydroxycarbene ligand either migrates to one of the metals or is eliminated along with one of the H atoms of the incoming molecule, presumably in the form of H_2 . In any case, the products obtained display invariably a *cis* arrangement of the newly generated CO group and the incoming ligand. Although we have detected no intermediate species in these reactions, the above results can be rationalized on the basis of the elementary steps collected in the Scheme 3.

The first step in all these reactions would be the coordination of the incoming ligand to the unsaturated dimetal center, which would occur preferentially at the less hindered position, that is,

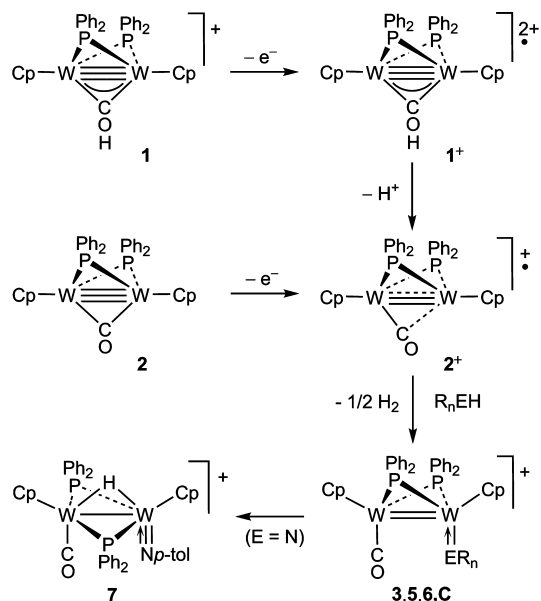
Scheme 3



between a PPh_2 group and the COH bridging ligand. This would leave the hydroxycarbene and the incoming molecule in a relative *cis* disposition (intermediate **A**), thus paralleling the carbonylation reactions of the bis(phosphide) complexes $[\text{M}_2\text{Cp}_2(\mu\text{-PR}'_2)_2(\mu\text{-CO})]$ ($\text{M} = \text{Mo}, \text{W}$; $\text{R} = \text{alkyl or aryl}$) to give specifically *cis*-dicarbonyl derivatives²⁰ and the addition of CO or isocyanides to the methoxycarbene complexes $[\text{M}_2\text{Cp}_2(\mu\text{-COMe})(\mu\text{-PR}'_2)_2]^+$ ($\text{M} = \text{Mo}, \text{R} = \text{Et}$; $\text{M} = \text{W}, \text{R} = \text{Ph}$).^{6a} We must note that the displacement of a related methoxycarbene ligand to an almost terminal position induced upon ligand coordination has been observed previously in the carbonylation of the unsaturated complex $[\text{Mo}_2\text{Cp}_2(\mu\text{-COMe})(\mu\text{-PCy}_2)(\mu\text{-CO})]$.^{7d} Under this view, the failure of phenol and *p*-toluidine to react with **1** possibly would be related to their poor donor properties, disfavoring the initial coordination step to give an intermediate of type **A**. The next step in these reactions would involve the transfer of the H atom of the hydroxycarbene ligand to the dimetal center, which in the case of PH_2Cy would directly give the final product **9**. This process would be analogous to the observed isomerization of the hydroxycarbene complex salts $[\text{Mo}_2\text{Cp}_2(\mu\text{-COH})(\mu\text{-PEt}_2)_2]\text{-BF}_4$ and $[\text{Mo}_2\text{Cp}_2(\mu\text{-COH})(\mu\text{-COMe})(\mu\text{-PCy}_2)]\text{BF}_4$ to give the corresponding hydride-carbonyl isomers.^{4a} However, the water and PhSH analogues of **9** (undetected complexes of type **B**) would not be stable enough, likely as a result of the still modest donor properties of these ligands. Instead, they would evolve rapidly via dehydrogenation to give the hydroxo (**3**) and thiolato (**6**) derivatives, respectively.

Pathways in the Redox-Induced Reactions of **1.** The phenolate and imido complexes **5** and **7** could only be obtained via one-electron oxidation of the neutral monocarbonyl **2**, in reactions that could not be replicated using the hydroxycarbene **1** as starting material. In fact, the reactions of the latter compound with these reagents led only to the oxohydride **4**, presumably as a consequence of the relatively larger amounts of trace water present in the reactions of **1**, due to the additional synthetic steps required to prepare this complex. However, the thiolato **6** could be obtained from either the hydroxycarbene **1** or the carbonyl **2** upon one-electron oxidation. Then, it seems reasonable to assume that the redox-induced reactions of **1** and **2** likely share a common intermediate (Scheme 4). Expectedly, the dicationic radical $\mathbf{1}^{\cdot+}$ following from the one-electron oxidation of the hydroxycarbene **1** would be extremely acidic, therefore being rapidly deprotonated (by the counterion or the added reagent), thus yielding a radical $\mathbf{2}^{\cdot+}$ identical to the one-electron oxidation product of the carbonyl-bridged complex **2**.

Scheme 4



Radical 2^+ thus would actually be the active species triggering the fast reactions of **1** and **2** with all HER_n molecules, including water. We have recently reported a related redox-induced chemistry of the benzylidyne complex $[\text{Mo}_2\text{Cp}_2(\mu\text{-CPh})(\mu\text{-PCy}_2)(\mu\text{-CO})]$.¹⁰ According to density functional theory (DFT) calculations, the removal of one electron in the latter complex yields a radical $[\text{Mo}_2\text{Cp}_2(\mu\text{-CPh})(\mu\text{-PCy}_2)(\mu\text{-CO})]^+$ with a weakened intermetallic bond and a linear semibridging carbonyl, while both the LUMO and most of the unpaired electron density are located at the same molybdenum atom, thus accounting for its reactivity toward simple HER_n reagents (thiols, phosphines, alcohols, etc.).¹⁰ To gain insight into the behavior of the radical 2^+ involved in the redox-induced reactions of **1** and **2**, we performed similar DFT²¹ calculations on both **2** and 2^+ (Table 3) (see Experimental Section and

Table 3. Selected Bond Lengths (Å) and Angles (deg) for the DFT-Optimized Structures of **2** and 2^+

	2	2^+		2	2^+
W1–W2	2.535	2.561	W1–P1–W2	63.5	63.8
W1–P1	2.409	2.430	W2–W1–C1	52.7	61.7
W2–P1	2.407	2.425	W1–W2–C1	52.8	47.1
W1–P2	2.407	2.418	P1–W1–C1	92.1	97.3
W–P2	2.409	2.418	W1–C1–O1	142.7	163.0
W1–C1	2.094	1.983	W2–C1–O1	142.8	125.8
W2–C1	2.092	2.381			
C1–O1	1.206	1.184			

Supporting Information for details). The emerging picture is similar to that of the benzylidyne complexes, with only minor differences. First, we found that the geometrical and electronic structure computed for **2** is comparable to that previously calculated for the dimolybdenum complex $[\text{Mo}_2\text{Cp}_2(\mu\text{-PEt}_2)_2(\mu\text{-CO})]^{4b}$ and deserves no particular comment, except to stress that the triple W–W bond in **2** can be similarly described as having one σ and two δ components (with one of the latter also having some bonding character to the bridging CO ligand), while the HOMO is a bonding orbital having σ Mo–CO character. The nature of these orbitals thus allow us

to understand that the removal of one electron from **2** involves a rearrangement of the carbonyl ligand and some weakening of the intermetallic interaction, the latter effect being against qualitative predictions based on the EAN formalism. Indeed, the optimized structure for 2^+ (Figure 2) displays a carbonyl

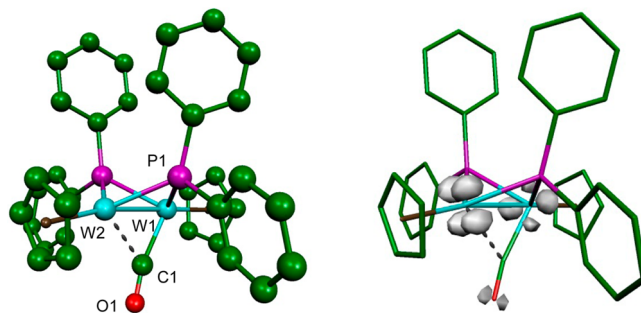


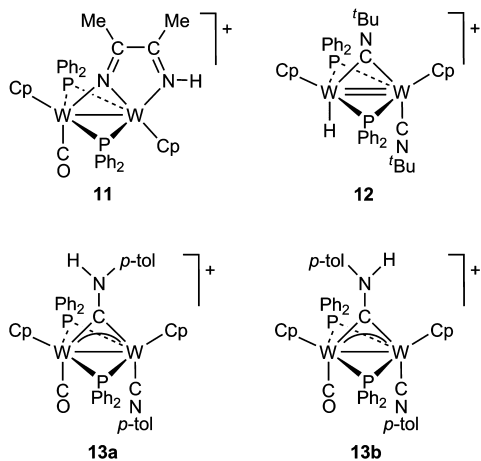
Figure 2. DFT-optimized structure of the cation in compound 2^+ with H atoms omitted (left) and total spin density for the same cation (right).

ligand in a linear semibridging fashion, weakly bound to the W2 atom ($\text{W2–C} = 2.381 \text{ Å}$), while the intermetallic distance of 2.561 Å is only ca. 0.03 Å longer than in the precursor **2** (2.535 Å). An analysis of the electron density in these molecules under the Atoms in Molecules theory²² gives a similar picture, with the density at the intermetallic bond critical point being just slightly reduced upon oxidation, from 0.665 (**2**) to 0.631 e Å^{-3} (2^+) (cf. 0.624 and 0.553 e Å^{-3} , respectively, in the benzylidyne complexes).¹⁰ Concerning its potential reactivity, we note that the LUMO in 2^+ is largely located at the dimetal center (actually having δ_{MM} bonding character, see the Supporting Information), so it is the total spin density, higher at the less protected W2 atom (Figure 2, right). This allows us to understand the reactivity of 2^+ toward HER_n molecules as centered at that metal atom, inducing the homolytic cleavage of the single E–H bonds to rapidly give ER_n derivatives with release of H atoms (Scheme 4). This would yield stable compounds except for the imido derivative $[\text{W}_2\text{Cp}_2(\mu\text{-PPh}_2)_2(\text{NH}p\text{-tol})(\text{CO})]\text{BF}_4$ (**C** in Scheme 4), which rapidly would undergo an oxidative addition of the N–H bond to give the imido hydride **7**, in a process completely analogous to the (slower) conversion of the hydroxycarbene **3** into its oxohydride isomer **4**.

Reactions of Compound 1 with Monodentate Ligands. In our previous studies on the reactivity of 30-electron methoxycarbene complexes we found that these unsaturated molecules are usually quite reactive toward simple two-electron donors such as CO or isocyanides, to give electron-precise derivatives in most cases.^{6,7d} Thus, we anticipated that compound **1** would react analogously. Indeed, although compound **1** failed to react with CO (1 atm) at room temperature, rapid reactions were observed with acetonitrile and isocyanides. However, all of these reactions involved the cleavage of the O–H bond of the hydroxycarbene ligand.

Compound **1** is instantaneously and selectively transformed into the α -diiminate complex salt $[\text{W}_2\text{Cp}_2(\mu\text{-PPh}_2)_2(\mu\text{-N:N,N'}\text{-N}_2\text{HC}_2\text{Me}_2)(\text{CO})]\text{BF}_4$ (**11**) by just dissolving it in acetonitrile (Chart 2). The formation of this compound involves the reductive C–C coupling of two acetonitrile molecules accompanied by transfer of the hydroxycarbene proton to one of the nitrogen atoms, to yield the diiminate ligand. There are several precedents for this relatively unusual coupling of

Chart 2



acetonitrile ligands.^{23,24} Of particular relevance, due to the similar coordination mode of the ligand generated, is the formation of the binuclear complexes: $[\text{Re}_2\text{X}_3(\mu\text{-N:N,N'-N}_2\text{HC}_2\text{Me}_2)(\mu\text{-dppm})_2(\text{NCMe})]\text{PF}_6$ ($\text{X} = \text{Cl}, \text{Br}$),²⁴ⁱ $[\text{W}_2(\mu\text{-NAr}')(\mu\text{-N:N,N'-N}_2\text{C}_2\text{Me}_2)(\text{OCMe}_2\text{CF}_3)_4]$ ($\text{Ar}' = \text{Xylil}$),^{24b} and $[\text{W}_2(\mu\text{-N:N,N'-N}_2\text{HC}_2\text{Me}_2)(\mu\text{-O}^i\text{Pr})_2(\text{O}^i\text{Pr})_5]$.^{24f} Yet, it is unusual that such reactions can take place under mild conditions, as observed for **11**. Although we have observed no intermediates in the formation of **11**, it is likely that this reaction might evolve initially through an unstable hydride intermediate similar to the phosphine complex **9**, which as a result of the poor donor properties of acetonitrile and its small size would add a second molecule of ligand, thus triggering the coupling and migration steps leading to **11**.

The reaction of **1** with isocyanides also involved the incorporation of two molecules of reagent but led to no C–C coupled products; moreover they were quite sensitive to the particular isocyanide used and even to the experimental conditions. Thus, compound **1** reacted rapidly with excess CN^tBu to give the 32-electron hydride $[\text{W}_2\text{Cp}_2(\text{H})(\mu\text{-PPh}_2)_2(\mu\text{-CN}^t\text{Bu})(\text{CN}^t\text{Bu})]\text{BF}_4$ (**12**) (Chart 2), a rather unstable product following from the addition of two isocyanide molecules, release of CO, and migration of the hydroxycarbene proton to one of the metal atoms. In contrast, the reaction with excess CN^ptol led to more stable products, identified as the electron-precise aminocarbene complex salt $[\text{W}_2\text{Cp}_2\{\mu\text{-CN}(\text{H})^p\text{tol}\}(\mu\text{-PPh}_2)_2(\text{CN}^p\text{tol})(\text{CO})]\text{BF}_4$ (**13**) (Chart 2), which is obtained as an equilibrium mixture of two isomers (**13a**/**13b**) differing in the orientation of the aminocarbene ligand in the asymmetric dimetal center (Chart 2). The formation of these products also requires the incorporation of two isocyanide molecules, but now decarbonylation does not take place, and the hydroxycarbene proton is eventually incorporated to one of the isocyanide molecules to yield an aminocarbene ligand. Interestingly, the reaction of **1** with stoichiometric amounts of CN^tBu gave a mixture of unreacted **1**, the hydride **12**, and several other species, two of which might be analogous to the isomers **13**, as judged from their similar ^{31}P NMR resonances. Unfortunately, we could not find experimental conditions to purify or prepare these products more selectively. In any case, these observations indicate that the structural differences between compounds **12** and **13** are not uniquely of thermodynamic origin but also derived from kinetic effects.

Structural Characterization of Compound 11. Although the quality of the crystals of compound **11** was very poor,

preventing a detailed analysis of the structural results, the connectivity and overall conformation of the molecule was confirmed through a single-crystal X-ray diffraction study (Figure 3).²⁵ The cation in **11** is built up from two transoid

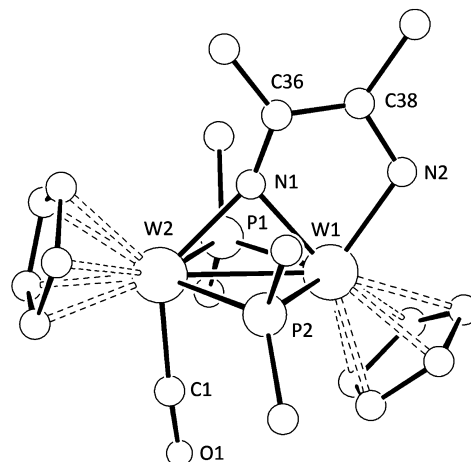


Figure 3. PLUTO diagram (30% probability) of the cation in compound **11** with H atoms and Ph groups (except their C¹ atoms) omitted.

WCp moieties connected by three bridging ligands: two PPh_2 ligands defining an almost flat W_2P_2 rhombus and the diiminate group, also binding one of the metal centers in a terminal way via its imine N atom. The coordination sphere of the other metal atom is completed with a carbonyl ligand slightly bent over the metal–metal bond. The intermetallic separation of 2.856(4) Å is relatively short for the single W–W bond that should be formulated for this 34-electron cation according to the EAN formalism, a fact that can be attributed to the presence of three bridging ligands, with one of them (N) having a small covalent radius. The overall arrangement of ligands in the cation of **11** implies that one of the metals exhibits the typical four-legged piano stool coordination geometry, while the second metal displays a less common trigonal bipyramidal environment. We have found this sort of geometry in different dicarbonyl complexes of the type $[\text{M}_2\text{Cp}_2(\mu\text{-PR}_2)(\mu\text{-X})(\mu\text{-Y})(\text{CO})_2]$ having three or more atoms bridging the dimetal unit.^{26,27} We finally note that the diiminate ligand displays an almost perfectly planar disposition, perpendicular to the Mo_2P_2 plane, analogous to those found in the Re_2 and W_2 complexes mentioned above.

The spectroscopic data in solution for **11** are consistent with the retention in solution of the solid-state structure. Thus, the presence of a terminal carbonyl ligand is clearly denoted by the appearance of a C–O stretching band at 1912 cm^{-1} in the corresponding IR spectrum and a deshielded ^{13}C NMR resonance at 227.3 ppm, while the equivalent PPh_2 bridging ligands give rise to a single ^{31}P resonance at –25.1 ppm. The latter represents a rather strong shielding for a PR_2 ligand bridging a M–M bond.²⁸ However, we have previously observed large ^{31}P nuclear shieldings in related 34-electron Mo_2 and W_2 cations of the type $[\text{M}_2\text{Cp}_2(\mu\text{-H})(\mu\text{-PR}_2)_2\text{L}_2]^+{}^8$ and $[\text{M}_2(\mu\text{-COMe})(\mu\text{-PR}_2)_2\text{L}_2]$,^{6a} also displaying flat M_2P_2 cores. As expected, the P–W couplings in **11** are much lower than in **1**, consistent with the increased number of donor atoms around the W atoms.¹² Finally, the presence of the diiminate ligand is denoted by the appearance of inequivalent CN (δ_{C}

159.7 and 153.9 ppm) and methyl resonances (δ_{C} 20.1 and 18.0 ppm). Although the nitrogen-bound H atom was not located in the crystallographic study, due to the low quality of the data, the presence of an N–H group is fully supported by the appearance of a characteristically deshielded resonance in the ^1H NMR spectrum (12.7 ppm) and also by the presence of a weak N–H stretching band at 3247 cm^{-1} in the corresponding solid-state IR spectrum.

Structural Characterization of Compound 12. The incorporation of two CN^tBu ligands in **12** is confirmed by the appearance of two ^tBu resonances with the expected intensities in the ^1H NMR spectrum. The equivalent PPh_2 groups give rise to a single ^{31}P NMR resonance at δ_{P} 60.5 ppm with substantially different one-bond P–W couplings ($J_{\text{PW}} = 319$ and 245 Hz), indicative of significant differences in the nature of the terminal ligands at the dimetal center. The migration of the hydroxycarbonyne proton to one of the metal atoms to form a terminal hydride ligand is firmly established by the appearance of a ^1H NMR resonance at 3.64 ppm, and the lack of diagnostic O–H or N–H bands in the solid-state IR spectrum. The unusually low shielding of this resonance is likely derived from the strong anisotropy of the double metal–metal bond that should be formulated for this cation according to the EAN formalism. For instance, we have shown previously that the resonance of the bridging hydride in the 32-electron cations $[\text{W}_2\text{Cp}_2(\mu\text{-H})(\mu\text{-PR}_2)(\mu\text{-Ph}_2\text{PCH}_2\text{PPh}_2)(\text{CO})_2]^{2+}$ ($\text{PR}_2 = \text{PPh}_2, \text{PhCy}$) is displaced from ca. -5 to $+3$ ppm by just exchanging the relative positions of the PR_2 and H ligands.²⁹

The IR spectrum of **12** displays two C–N stretching bands at 2140 and 1950 cm^{-1} . The more energetic band is characteristic of terminal isocyanide ligands with a linear disposition in a cationic complex (**I** in Chart 3), a proposal consistent with the

$220\text{--}240\text{ ppm}$ for the type **II** ligands in complexes $[\text{MoCp}_2(\text{CNR})]^{34}$ and $[\text{WCp}^*(\text{CNR})_2(\text{CNEt}_2)]$.³⁵ Thus a linear bridging coordination is proposed for the second isocyanide ligand in **12**, which in turn is consistent with the presence of a terminal hydride in the molecule.

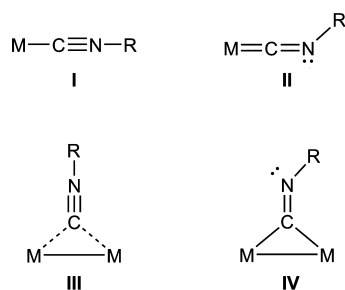
We should note that, in any case, the structure of **12** is highly unexpected after considering that related Mo_2 and W_2 hydrides previously reported invariably display hydride-bridged structures of the type $[\text{M}_2\text{Cp}_2(\mu\text{-H})(\mu\text{-PR})_2\text{L}_2]^+$ with terminal L ligands ($\text{L} = \text{CO}, \text{CN}^t\text{Bu}$) arranged almost parallel to each other, these including the crystallographically characterized cations $[\text{W}_2\text{Cp}_2(\mu\text{-H})(\mu\text{-PPh}_2)_2(\text{CO})_2]^+$ and $[\text{Mo}_2\text{Cp}_2(\mu\text{-H})(\mu\text{-PCy}_2)_2(\text{CO})(\text{CN}^t\text{Bu})]^+$.⁸ The phosphine hydride **9** still represents a third isomeric form in this family of 32-electron binuclear hydrides, as noted above. At present, however, we cannot give a satisfactory explanation for the observed structural preferences in these unsaturated hydrides.

Structural Characterization of the Aminocarbonyne Complex 13.

The spectroscopic data for both isomers of compound **13** are similar to each other (Table 1 and Experimental Section), therefore indicating a close structural relationship. Their ^{31}P NMR spectra display a single and strongly shielded resonance at ca. -25 ppm in each case, which seems to be a characteristic feature of cations of the type $[\text{M}_2\text{Cp}_2(\mu\text{-X})(\mu\text{-PR}_2)_2\text{L}_2]^+$ having flat M_2P_2 cores, as noted above (cf. -25.1 ppm for **11**). The presence of a terminal isocyanide ligand in each case is denoted by the appearance of a high frequency C–N stretch at ca. 2110 cm^{-1} in the IR spectrum and a poorly deshielded resonance at ca. 165 ppm in the $^{13}\text{C}\{^1\text{H}\}$ NMR spectrum. In contrast, the aminocarbonyne ligands display a much more deshielded ^{13}C resonance at ca. 315 ppm . For comparison, we note that the latter figures are quite similar to those measured in related aminocarbonyne complexes such as $[\text{W}_2\text{Cp}_2(\mu\text{-CNHMe})(\mu\text{-H})(\text{CO})_4]$ (317.4 ppm)³⁶ and in the crystallographically characterized $[\text{W}_2\text{Cp}_2\{\mu\text{-CNH}(\text{Xyl})\}(\mu\text{-PCy}_2)(\text{CO})(\text{CNXyl})]$ (ca. 336 ppm).³⁷ The carbonyl ligand in the isomers of **13** gives rise to a strong C–O stretching band at 1960 cm^{-1} and a deshielded ^{13}C resonance at ca. 230 ppm , as expected. Finally, the presence of a N–H bond in these complexes is deduced from the appearance of a deshielded ^1H NMR resonance at ca. 9.4 ppm and a characteristic high-frequency band in the solid-state IR spectrum (3310 cm^{-1}).

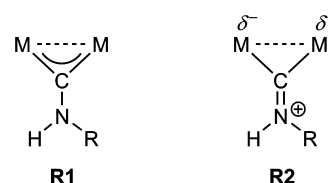
To explain the presence of isomers in the solutions of **13**, we must recall that the structure and electronic distribution within aminocarbonyne ligands typically is best described by the contribution of two canonical forms: an aminocarbonyne form involving π bonding between C and the metal atoms (**R1**) and an iminium-type form (**R2**) involving π bonding between the C and N atoms (Chart 4).³⁸ This implies that the rotation around the C–N bond in these complexes is restricted, thus allowing for the existence of two slowly interconverting isomers if the

Chart 3



presence of a moderately deshielded resonance at 199.0 ppm in the ^{13}C NMR spectrum. The less energetic C–N stretch might be associated with at least two coordination modes of the isocyanide ligand: either a bent terminal mode (**II** in Chart 3) usually leading to C–N stretches in the range $1800\text{--}1900\text{ cm}^{-1}$ or a linear bridging mode (**III** in Chart 3), with the bent bridging mode (**IV** in Chart 3) being discarded since it usually leads to less energetic C–N stretches (in the range $1580\text{--}1880\text{ cm}^{-1}$).³⁰ Indeed, the complexes $[\text{Pd}_2\text{Cl}_2\{\mu\text{-CN}(2,6\text{-C}_6\text{H}_3\text{Me}_2)\}_2(\text{py})_2]$,³¹ $[\text{Pd}_2(\eta^5\text{-C}_5\text{Ph}_5)\{\mu\text{-CN}(2,6\text{-C}_6\text{H}_3\text{Me}_2)\}_2]$,³² and $[\text{Pd}_4(\mu\text{-OAc})_4(\mu\text{-CN}^t\text{Bu})_4]$,³³ all of them having linear bridging CNR groups (as determined by crystallographic studies), exhibit C–N stretches in the range $1956\text{--}1976\text{ cm}^{-1}$. On the other hand, the high chemical shift for the second isocyanide ligand in **12** (δ_{C} 255.1 ppm) gives a slightly better match with a coordination of type **III** (cf. $220\text{--}260\text{ ppm}$ for different complexes with type **III** ligands,³⁰ but

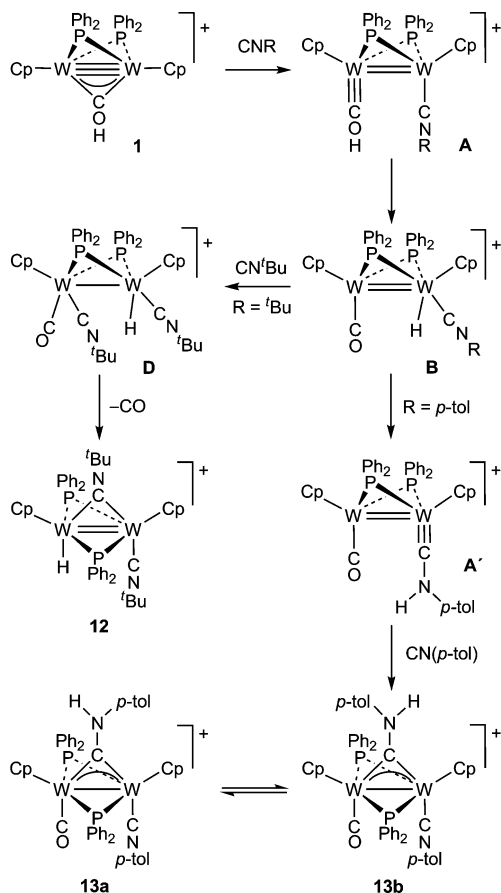
Chart 4



two metal centers are otherwise inequivalent, as is the case with compound 13.

Pathways in the Reactions of Compound 1 with Isocyanides. Although we have detected no intermediates in the reactions of **1** with isocyanides, the nature of the products obtained can be rationalized by considering the participation of species related to those proposed for the reactions with HER_n molecules discussed above (Scheme 5). The first two steps

Scheme 5



would analogously involve coordination of a molecule of reagent to yield a hydroxycarbene intermediate of type **A**, followed by migration of the hydroxycarbene proton to one of the metals, then rendering a hydride intermediate **B** structurally related to the phosphine complex **9**. From here on, the evolution of these intermediates would depend critically on the particular isocyanide. For the more basic CN^tBu ligand, the coordination of a second isocyanide molecule would be fast when present in excess, before any rearrangement can possibly take place, then giving a bis(isocyanide) intermediate **D** that would evolve to the final product **12** after spontaneous decarbonylation and terminal to bridging rearrangement of a isocyanide ligand. The less basic $\text{CN}^p\text{-tol}$ ligand would react more slowly, so that the insertion of the coordinated isocyanide in the $\text{M}-\text{H}$ bond at intermediate **B** might occur before a second molecule of ligand reaches the dimetal center, thus yielding a carbonyl/aminocarbene intermediate **A'** analogous to the isocyanide/hydroxycarbene intermediate **A**, which then would add the second $\text{CN}^p\text{-tol}$ molecule to eventually give the final product **13**, in a process comparable to those observed in the reactions of the methoxycarbene cations $[\text{M}_2\text{Cp}_2(\mu-$

$\text{COMe})(\mu\text{-PR}_2)_2]^+$ ($\text{M} = \text{W}$, $\text{R} = \text{Ph}$; $\text{M} = \text{Mo}$, $\text{R} = \text{Et}$) with CN^tBu .^{6a} This second pathway would also be operative at some extent when using stoichiometric amounts of CN^tBu in these reactions, as noted above. We should finally note that although the insertion of isocyanide ligands in $\text{M}-\text{H}$ bonds is well-documented in reactions of molecules having unsaturated M_2H centers, these processes usually lead to formimidoyl derivatives ($-\text{C}(\text{H})\text{NR}$).³⁹ However, there is a number of instances where the isolated products of these reactions are the corresponding aminocarbene derivatives,^{36–38,39a} presumably formed in some cases through deprotonation/protonation processes, a mechanism that cannot be excluded for the cationic intermediates of type **B**.

CONCLUSION

The reactivity of the hydroxycarbene complex salt $[\text{W}_2\text{Cp}_2(\mu\text{-COH})(\mu\text{-PPh}_2)_2]\text{BF}_4$ (**1**) invariably involves the cleavage of its $\text{O}-\text{H}$ bond, to give products strongly dependent on the added reagent and experimental conditions. Most of the reactions with potential donor molecules **L** seem to be initiated with the coordination of **L** to the unsaturated cation and H -transfer of the hydroxycarbene proton to the dimetal site, to give 32-electron hydride carbonyl complexes of the type $[\text{W}_2\text{Cp}_2(\text{H})(\mu\text{-PPh}_2)_2(\text{CO})\text{L}]^+$, which are stable only when **L** is a phosphine ligand. When **L** is an HER_n molecule such as H_2O and HSPh , then cleavage of the $\text{E}-\text{H}$ bond also takes place to give hydroxo and thiolato derivatives of the type $[\text{W}_2\text{Cp}_2(\text{ER}_n)(\mu\text{-PPh}_2)_2(\text{CO})]^+$ and hydrogen. These reactions are greatly accelerated in the presence of stoichiometric amounts of the oxidant $[\text{FeCp}_2]\text{BF}_4$ and can be replicated under the latter conditions when using the carbonyl-bridged complex $[\text{W}_2\text{Cp}_2(\mu\text{-PPh}_2)_2(\mu\text{-CO})]$ (**2**) instead. This equivalence can be explained by assuming that the dication following from one-electron oxidation of **1** would be extremely acidic and therefore rapidly deprotonated to give a radical $[\text{W}_2\text{Cp}_2(\mu\text{-PPh}_2)_2(\mu\text{-CO})]^+$ (**2⁺**) identical to that following from the one-electron oxidation of **2**. Radical **2⁺** displays a slightly weakened intermetallic bond and a linear semibridging carbonyl, according to DFT calculations; moreover, both the LUMO and most of the unpaired electron density in this cation are located at the dimetal center, thus explaining its fast induction of $\text{E}-\text{H}$ bond cleavages when faced to HER_n molecules, to give $[\text{W}_2\text{Cp}_2(\text{ER}_n)(\mu\text{-PPh}_2)_2(\text{CO})]^+$ derivatives ($\text{ER}_n = \text{OH}$, SPh , OPh , $\text{NH}^p\text{-tol}$) and hydrogen. When $\text{L} = \text{NCMe}$ or CNR , however, the $[\text{W}_2\text{Cp}_2(\text{H})(\mu\text{-PPh}_2)_2(\text{CO})\text{L}]^+$ intermediates evolve through the addition of a second molecule of **L**, in processes strongly dependent on **L** and experimental conditions, usually accompanied by H -transfer to **L** and other rearrangements, such as the reductive $\text{C}-\text{C}$ coupling between acetonitrile molecules, to give products containing aminocarbene or diiminate ligands, as exemplified by the formation of the complexes $[\text{W}_2\text{Cp}_2\{\mu\text{-CN}(\text{H})^p\text{-tol}\}(\mu\text{-PPh}_2)_2(\text{CN}^p\text{-tol})(\text{CO})]^+$ and $[\text{W}_2\text{Cp}_2(\mu\text{-PPh}_2)_2(\mu\text{-N:N,N',N'-N}_2\text{HC}_2\text{Me}_2)(\text{CO})]^+$ respectively.

EXPERIMENTAL SECTION

General Procedures. All reactions and manipulations were carried out under a nitrogen atmosphere using standard Schlenk techniques. Solvents were purified according to literature procedures⁴⁰ and distilled under nitrogen prior to use. Petroleum ether refers to that fraction distilling in the range 338–343 K. Compounds $[\text{W}_2\text{Cp}_2(\mu\text{-COH})(\mu\text{-PPh}_2)_2]\text{BF}_4$ (**1**),¹ $[\text{W}_2\text{Cp}_2(\mu\text{-PPh}_2)_2(\mu\text{-CO})]$ (**2**),²⁰ and $[\text{FeCp}_2]\text{BF}_4$ ⁴¹ were prepared as described previously. All other

reagents were obtained from the usual commercial suppliers and used as received. Filtrations were carried out through diatomaceous earth. Chromatographic separations were carried out using jacketed columns cooled by tap water (ca. 288 K) or kept at the desired temperature with a cryostat. Commercial aluminum oxide (Aldrich, activity I, 150 mesh) was degassed under vacuum prior to use. The latter was afterward mixed under nitrogen with the appropriate amount of water to reach the activity desired. IR stretching frequencies of C–O, C–N, N–H, and B–F bonds were measured either in solution (using CaF₂ windows) or in Nujol mulls (using NaCl windows), are referred to as $\nu(\text{CO})$, $\nu(\text{CN})$, $\nu(\text{NH})$, or $\nu(\text{BF})$, and are given in cm^{−1}. Nuclear magnetic resonance (NMR) spectra were routinely recorded at 300.13 (¹H), 75.46 MHz (¹³C{¹H}), and 121.50 MHz (³¹P{¹H}) at 290 K in CD₂Cl₂ solutions unless otherwise stated. Chemical shifts (δ) are given in ppm, relative to internal tetramethylsilane (¹H, ¹³C) or external 85% aqueous H₃PO₄ solutions (³¹P). Coupling constants (*J*) are given in hertz.

Preparation of [W₂Cp₂(OPh)(μ -PPh₂)₂(CO)]BF₄ (5). Freshly sublimed phenol (ca. 0.050 g, 0.532 mmol) and [FeCp₂]BF₄ (0.009 g, 0.033 mmol) were added to a solution of compound 2 (0.030 g, 0.033 mmol) in dichloromethane (10 mL). The mixture was stirred for 10 min to give a green solution containing compound 5 as the only P-containing organometallic product. Unfortunately, compound 5 could not be isolated as a pure material because of its progressive hydrolysis upon manipulation (to give compounds 3 and 4), and all spectroscopic data were obtained from these crude reaction mixtures. ¹H NMR (200.13 MHz): δ 7.91–7.32 (m, 25 H, PPh and OPh), 5.83, 5.50 (2s, 2 \times 5H, Cp).

Preparation of [W₂Cp₂(μ -H)(Np-tol)(μ -PPh₂)₂(CO)]BF₄ (7). Solid *p*-toluidine (0.004 g, 0.037 mmol) was dried by heating under vacuum and then mixed with a solution of 2 (0.030 g, 0.033 mmol) in dichloromethane (10 mL). The mixture was stirred for 5 min, and then solid [FeCp₂]BF₄ (0.009 g, 0.033 mmol) was added, whereupon the solution turned orange immediately. The solution was then filtered, petroleum ether (10 mL) was added, and the solvents were partially removed under vacuum until most of the product precipitated. The remaining solution was discarded, and the resulting orange solid was washed with petroleum ether (2 \times 10 mL) and dried under vacuum to give compound 7 as an orange solid (0.028 g, 78%). The crystals used in the X-ray study were grown through the slow diffusion of a diethyl ether/petroleum ether (1:1) mixture into a dichloromethane solution of the compound at room temperature. Anal. Calcd for C₄₂H₃₈BF₄NOP₂W₂: C, 46.31; H, 3.52; N, 1.29. Found: C, 46.13; H, 3.60; N, 1.39. ¹H NMR: δ 7.66 (m, 4H, PPh), 7.48 (m, 4H, PPh), 7.40–7.22 (m, 12H, PPh), 6.82, 6.05 (2 false d, 2 \times 2H, *J*_{HH} = 8, C₆H₄), 5.85, 5.49 (2s, 2 \times 5H, Cp), 2.16 (s, 3H, Me), −9.18 (t, 1H, *J*_{HP} = 52, *J*_{HW} = 34, μ -H). The value of the *J*_{HW} coupling of the hydride resonance with the second metal center was estimated (from the line width of this resonance) to be lower than 9 Hz.

Preparation of [W₂Cp₂(Np-tol)(μ -PPh₂)₂(CO)] (8). Neat 1,8-diazabicycloundec-7-ene (DBU, 25 μ L, 0.167 mmol) was added to a solution of compound 7 (0.020 g, 0.018 mmol) in dichloromethane (10 mL), and the resulting mixture was stirred for 10 min to give a red solution. The solvent was then removed under vacuum, and the residue was chromatographed on alumina (activity IV) at 288 K. Elution with dichloromethane/petroleum ether (2:1) gave a deep red fraction yielding, after removal of the solvents, compound 8 as a red solid (0.017 g, 94%). Anal. Calcd for C₄₂H₃₇NOP₂W₂: C, 50.38; H, 3.72; N, 1.40. Found: C, 50.73; H, 3.87; N, 1.45. ¹H NMR (200.13 MHz): δ 7.85 (m, 4H, PPh), 7.31–7.18 (m, 12H, PPh), 6.89 (m, 4H, PPh), 6.48, 5.64 (2 false d, 2 \times 2H, *J*_{HH} = 8, C₆H₄), 5.23, 5.14 (2s, 2 \times 5H, Cp), 1.90 (s, 3H, Me).

Preparation of [W₂Cp₂(H)(μ -PPh₂)₂(CO)(PH₂Cy)]BF₄ (9). Cyclohexylphosphine (18 μ L, 0.14 mmol) was added to a solution of compound 1 (0.070 g, 0.071 mmol) in dichloromethane (10 mL), and the mixture was stirred for 4 h to give a green solution containing compound 9 and small amounts of 4. The solution was then filtered, and the solvent was removed from the filtrate. Recrystallization of this crude product from dichloromethane/petroleum ether gave green crystals of 9, which were washed with petroleum ether and dried under

vacuum (0.050 g, 64%). Anal. Calcd for C₄₁H₄₄BF₄OP₂W₂: C, 44.76; H, 4.03. Found: C, 44.31; H, 3.70. IR (Nujol): $\nu(\text{PH})$ 2363 (w); $\nu(\text{CO})$ 1893 (s); $\nu(\text{BF})$ 1050 (s, br). ¹H NMR: δ 8.11, 7.88 (2m, 2 \times 2H, PPh), 7.69–7.29 (m, 12H, PPh), 6.82, 6.73 (2m, 2 \times 2H, PPh), 5.57, 4.91 (2s, 2 \times 5H, Cp), 4.78 (d, *J*_{HP} = 365, 2H, PH₂), 1.54–0.66 (m, 11H, Cy), −0.79 (ddd, *J*_{HP} = 67, 36, 11, 1H, W–H).

Preparation of [W₂Cp₂(μ -PPh₂)₂(CO)(PH₂Cy)] (10). The procedure and workup was analogous to that described for 8, but using compound 9 (0.050 g, 0.045 mmol) and 30 μ L of DBU (0.200 mmol). Elution with petroleum ether gave a pale green fraction yielding, after removal of solvent, compound 10 as a green solid (0.043 g, 94%). Anal. Calcd for C₄₁H₄₃OP₂W₂: C, 48.64; H, 4.28. Found: C, 48.20; H, 4.17. IR (Nujol): $\nu(\text{PH})$ 2290 (w); $\nu(\text{CO})$ 1858 (s). ¹H NMR (200.13 MHz): δ 7.92 (m, 4H, PPh), 7.47–7.28 (m, 6H, PPh), 7.17–7.01 (m, 6H, PPh), 6.64 (m, 4H, PPh), 4.83 (s, 5H, Cp), 4.51 (dt, *J*_{HP} = 3.5, 1, 5H, Cp), 3.89 (dm, *J*_{HP} = 340, 2H, PH₂), 1.35–0.30 (m, 11H, Cy).

Preparation of [W₂Cp₂(μ -PPh₂)₂(μ -N,N,N'-N₂HC₂Me₂)(CO)]BF₄ (11). Compound 1 (0.030 g, 0.030 mmol) was dissolved in freshly distilled acetonitrile (10 mL) and stirred for 5 min. The resulting orange solution was then filtered, petroleum ether (10 mL) was added, and the solvents were partially removed under vacuum until most of the product precipitated. The remaining solution was discarded, and the resulting orange solid was washed with petroleum ether (2 \times 10 mL) and dried under vacuum to give compound 11 as an orange solid (0.029 g, 83%). The crystals used in the X-ray study were grown through the slow diffusion of a toluene/petroleum ether (1:1) mixture into a dichloromethane solution of the compound at room temperature. Anal. Calcd for C₃₉H₃₇BF₄N₂OP₂W₂: C, 43.94; H, 3.50; N, 2.63. Found: C, 43.67; H, 3.64; N, 2.37. IR (Nujol): $\nu(\text{NH})$ 3347 (w); $\nu(\text{CO})$ 1913 (s); $\nu(\text{CN})$ 1506 (w); $\nu(\text{BF})$ 1050 (s, br). ¹H NMR: δ 12.7 (s, 1H, NH), 7.70–7.10 (m, 16H, Ph), 6.58 (m, 4H, Ph), 6.02, 5.27 (2s, 2 \times 5H, Cp), 2.19 (s, 3H, Me), 0.66 (t, 3H, *J*_{HP} = 5, Me). ¹³C{¹H} NMR: δ 227.3 (s, WCO), 159.7 (s, WNC), 153.9 (t, *J*_{CP} = 8, WNC), 136.7–126.5 (m, Ph), 95.3, 88.1 (2s, Cp), 20.1, 18.0 (2s, Me).

Preparation of [W₂Cp₂(H)(μ -PPh₂)₂(μ -CN^tBu)(CN^tBu)]BF₄ (12). A dichloromethane solution (8 mL) of CN^tBu (10 μ L, 0.090 mmol) was placed in a dropping funnel and then added slowly to a solution of compound 1 (0.030 g, 0.030 mmol) in dichloromethane (10 mL) cooled at 263 K. The resulting orange solution was further stirred for 10 min, and then diethyl ether (10 mL) was added. The solvents were partially removed under vacuum until most of the product precipitated, and the remaining solution was discarded. The resulting orange solid was washed with diethyl ether (2 \times 10 mL) and dried under vacuum (0.031 g, 91%) to give compound 12 as an essentially pure orange solid. Attempts to further purify this air-sensitive material resulted in its progressive decomposition; therefore, no satisfactory elemental analysis was obtained for this compound. ¹H NMR: δ 7.75–7.17 (m, 20H, Ph), 5.98, 5.15 (2s, 2 \times 5H, Cp), 3.64 (s, br, 1H, W–H), 1.01, 0.76 (2s, 2 \times 9H, ^tBu). ¹H NMR (400.13 MHz, 213 K): δ 7.76–7.26 (m, 20H, Ph), 6.11, 5.18 (2s, 2 \times 5H, Cp), 3.85 (s, 1H, W–H), 0.95, 0.70 (2s, 2 \times 9H, ^tBu). ¹³C{¹H} NMR (100.61 MHz, 213 K): δ 255.1 (s, μ -CN^tBu), 199.0 (s, WCN^tBu), 144.7, 141.4 [2m, AXX', C¹(Ph)], 134.1–128.2 (m, Ph), 93.8, 87.1 (2s, Cp), 59.9, 52.6 [2s, C¹(^tBu)], 30.0, 29.4 [2s, C²(^tBu)].

Preparation of [W₂Cp₂(μ -CN(H)*p*-tol)(μ -PPh₂)₂(CN*p*-tol)(CO)]BF₄ (13). The procedure and workup was analogous to that described for 12 but using *p*-tolylisocyanide (0.011g, 0.093 mmol) and a reaction temperature of 273 K. This yielded compound 13 as an orange solid (0.033 g, 90%). In solution, compound 13 was present as an equilibrium mixture of two isomers 13a and 13b, with their ratio being solvent-dependent [a/b ratio ca. 2:1 in CD₂Cl₂ and 5:4 in Me₂CO-*d*₆ solution]. Anal. Calcd for C₅₁H₄₅BF₄N₂OP₂W₂: C, 50.28; H, 3.72; N, 2.30. Found: C, 49.87; H, 3.44; N, 2.11. IR (Nujol): $\nu(\text{NH})$ 3311 (w), $\nu(\text{CN})$ 2110 (vs), $\nu(\text{CO})$ 1949 (s), $\nu(\text{BF})$ 1055 (vs, br). Spectroscopic data for 13a: ¹H NMR (200.13 MHz): δ 9.37 (s, br, 1H, NH), 7.62 (m, 4H, Ph), 7.37–7.22 (m, 12H, Ph), 6.91 (m, 4H, Ph), 5.89, 5.51 (2m, 2 \times 2H, C₆H₄), 5.72, 5.23 (2s, 2 \times 5H, Cp), 2.28, 2.24 (2s, 2 \times 3H, Me). ¹³C{¹H} NMR (100.61 MHz, Me₂CO-*d*₆): δ

315.7 (t, $J_{\text{PC}} = 41$, $\mu\text{-CN}$), 230.2 (t, $J_{\text{PC}} = 7$, WCO), 168.1 (t, $J_{\text{PC}} = 8$, WCN), 143.9–126.3 (m, Ph and C_6H_4), 90.3, 89.5 (2s, Cp), 21.1, 20.9 (2s, Me). Spectroscopic data for **13b**: ^1H NMR (200.13 MHz): δ 9.37 (s, br, 1H, NH), 7.62 (m, 4H, Ph), 7.37–7.22 (m, 12H, Ph), 6.91 (m, 4H, Ph), 5.96, 5.53 (2m, $2 \times 2\text{H}$, C_6H_4), 5.68, 5.17 (2s, $2 \times 5\text{H}$, Cp), 2.28, 2.25 (2s, $2 \times 3\text{H}$, Me). $^{13}\text{C}\{^1\text{H}\}$ NMR (100.61 MHz, $\text{Me}_2\text{CO}-d_6$): δ 312.6 (t, $J_{\text{PC}} = 41$, $\mu\text{-CN}$), 226.2 (t, $J_{\text{PC}} = 7$, WCO), 164.3 (t, $J_{\text{PC}} = 8$, WCN), 143.9–126.3 (m, Ph and C_6H_4), 90.6, 88.9 (2s, Cp), 21.1, 20.9 (2s, Me).

Computational Details. The computations for compounds **2** and **2*** were carried out using the GAUSSIAN03 package,⁴² in which the hybrid methods B3LYP (**2**) and UB3LYP (**2***) were applied with the Becke three parameters exchange functional⁴³ and the Lee–Yang–Parr correlation functional.⁴⁴ An accurate numerical integration grid (99,590) was used for all calculations via the keyword Int=Ultrafine. Effective core potentials (ECP) and their associated double- ζ LANL2DZ basis set were used for the metal atoms.⁴⁵ The light elements (P, O, C, and H) were described with the 6-31G* basis set.⁴⁶ Geometry optimizations were performed under no symmetry restrictions, using initial coordinates derived from the X-ray data of the Mo analogue of **2**, and frequency analysis was performed to ensure that a minimum structure with no imaginary frequencies was achieved in each case. Molecular orbitals and vibrational modes were visualized using the MOLEKEL program.⁴⁷ The topological analysis of the electron density was carried out with the Xaim routine.⁴⁸

X-ray Structure Determination of Compound 7. The diffraction data for this compound were collected at 293 K on a Siemens AED single-crystal diffractometer, using Mo $K\alpha$ graphite monochromated radiation ($\lambda = 0.71073$ Å). The structure was solved by direct methods with SHELXS-97⁴⁹ and refined against F^2 with SHELXL-97,⁵⁰ with anisotropic thermal parameters for all non hydrogen atoms. The hydrogen atoms were placed in the ideal geometrical positions. The hydride H1 atom was found in the ΔF map. Details of the X-ray diffraction collection are reported in Table S8 in Supporting Information.

■ ASSOCIATED CONTENT

● Supporting Information

CIF file giving the crystallographic data for the structural analysis of compound **7**; PDF file containing data (complete ref 42, figures, selected bond distances and angles, selected molecular orbitals, atomic charges and topological properties of the electron density) for the DFT-optimized structures of **2** and **2***, and a table with crystal data of compound **7**. This material is available free of charge via the Internet at <http://pubs.acs.org>.

■ AUTHOR INFORMATION

Corresponding Author

*E-mail: mar@uniovi.es.

Notes

The authors declare no competing financial interest.

■ ACKNOWLEDGMENTS

We thank the DGI of Spain (Projects CTQ2009-09444 and CTQ2012-33187) and the European Commission (Project PERG08-GA-2010-276958) for supporting this work and the Consejería de Educación of Asturias for a “Clarín” postdoctoral reintegration grant (D.G.V.).

■ REFERENCES

- (1) García, M. E.; Riera, V.; Rueda, M. T.; Ruiz, M. A.; Halut, S. J. *Am. Chem. Soc.* **1999**, *121*, 1960.
- (2) The first thermally stable hydroxycarbyne complex reported was the 32-electron species $[\text{W}_2\text{Cp}_2(\mu\text{-COH})(\mu\text{-Ph}_2\text{PCH}_2\text{PPh}_2)(\text{CO})_2]\text{BF}_4$; see: (a) Alvarez, M. A.; García, M. E.; Riera, V.; Ruiz, M. A.; Robert, F. *Organometallics* **2002**, *21*, 1177. (b) Alvarez, M. A.; García, M. E.; Riera, V.; Ruiz, M. A. *Organometallics* **1999**, *18*, 634. (c) Alvarez, M. A.; Bois, C.; García, M. E.; Riera, V.; Ruiz, M. A. *Angew. Chem., Int. Ed. Engl.* **1996**, *35*, 102.
- (3) (a) García, M. E.; Melón, S.; Ramos, A.; Ruiz, M. A. *Dalton Trans.* **2009**, 8171. (b) García, M. E.; Melón, S.; Ramos, A.; Riera, V.; Ruiz, M. A.; Belletti, D.; Graiff, C.; Tiripicchio, A. *Organometallics* **2003**, *22*, 1983. (c) Alvarez, M. A.; García, M. E.; García-Vivó, D.; Ruiz, M. A.; Vega, M. F. *Organometallics* **2010**, *29*, 512.
- (4) (a) García, M. E.; García-Vivó, D.; Ruiz, M. A.; Alvarez, S.; Aullón, G. *Organometallics* **2007**, *26*, 4930. (b) Alvarez, C. M.; Alvarez, M. A.; García, M. E.; García-Vivó, D.; Ruiz, M. A. *Organometallics* **2005**, *24*, 4122.
- (5) Alvarez, M. A.; García, M. E.; Martínez, M. E.; Menéndez, S.; Ruiz, M. A. *Organometallics* **2010**, *29*, 710.
- (6) (a) García, M. E.; García-Vivó, D.; Ruiz, M. A.; Herson, P. *Organometallics* **2008**, *27*, 3879. (b) García, M. E.; García-Vivó, D.; Ruiz, M. A. *Organometallics* **2008**, *27*, 543.
- (7) (a) García, M. E.; García-Vivó, D.; Ruiz, M. A. *Organometallics* **2010**, *29*, 2157. (b) García, M. E.; García-Vivó, D.; Ruiz, M. A. *Organometallics* **2009**, *28*, 4385. (c) García, M. E.; García-Vivó, D.; Ruiz, M. A. *Organometallics* **2008**, *27*, 169. (d) García, M. E.; García-Vivó, D.; Ruiz, M. A.; Aullón, G.; Alvarez, S. *Organometallics* **2007**, *26*, 5912.
- (8) Alvarez, M. A.; García, M. E.; Martínez, M. E.; Ramos, A.; Ruiz, M. A.; Sáez, D. *Inorg. Chem.* **2006**, *45*, 6965.
- (9) (a) Maitlis, P. M.; Zanotti, V. *Chem. Commun.* **2009**, 1619. (b) Maitlis, P. M. *J. Organomet. Chem.* **2004**, *689*, 4366. (c) Maitlis, P. M. *J. Mol. Catal. A* **2003**, *204* (205), 55. (d) Dry, M. E. *Catal. Today* **2002**, *71*, 227.
- (10) Alvarez, M. A.; García, M. E.; García-Vivó, D.; Menéndez, S.; Ruiz, M. A. *Organometallics* **2013**, *32*, 218.
- (11) Cimadevilla, F.; García, M. E.; García-Vivó, D.; Ruiz, M. A.; Graiff, C.; Tiripicchio, A. *Inorg. Chem.* **2012**, *51*, 10427.
- (12) Jameson, C. J. In *Phosphorus-31 NMR Spectroscopy in Stereochemical Analysis*; Verkade, J. G., Quin, L. D., Eds.; VCH: Deerfield Beach, FL, 1987; Chapter 6.
- (13) Curtis, M. D.; Hay, M. S.; Butler, W. M.; Kampf, J.; Rheingold, A. L.; Haggerty, B. S. *Organometallics* **1992**, *11*, 2884.
- (14) Gómez Sal, P.; Jiménez, I.; Martín, A.; Pedraz, T.; Royo, P.; Sellés, A.; Vázquez de Miguel, A. *Inorg. Chim. Acta* **1998**, *273*, 270.
- (15) Li, L.; White, P. S.; Brookhart, M.; Templeton, J. L. *J. Am. Chem. Soc.* **1990**, *112*, 8190.
- (16) Danopoulos, A. A.; Redshaw, C.; Vaniche, A.; Wilkinson, G.; Hussain-Bates, B.; Hursthouse, M. B. *Polyhedron* **1993**, *12*, 1061.
- (17) Pétillon, F. Y.; Schollhammer, P.; Talarmin, J.; Muir, K. W. *Coord. Chem. Rev.* **1998**, *178–180*, 203.
- (18) Cimadevilla, F.; García, M. E.; García-Vivó, D.; Ruiz, M. A.; Graiff, C.; Tiripicchio, A. *Inorg. Chem.* **2012**, *51*, 7284.
- (19) Wrackmeyer, B.; Alt, H. G.; Maisel, H. E. *J. Organomet. Chem.* **1990**, *399*, 125.
- (20) García, M. E.; Riera, V.; Ruiz, M. A.; Rueda, M. T.; Sáez, D. *Organometallics* **2002**, *21*, 5515.
- (21) (a) Koch, W.; Holthausen, M. C. *A Chemist's Guide to Density Functional Theory*, 2nd ed.; Wiley-VCH: Weinheim, Germany, 2002. (b) Ziegler, T. *Chem. Rev.* **1991**, *91*, 651. (c) Foresman, J. B.; Frisch, A. E. *Exploring Chemistry with Electronic Structure Methods*, 2nd ed.; Gaussian, Inc.: Pittsburg, 1996.
- (22) Bader, R. F. W. *Atoms in Molecules—A Quantum Theory*; Oxford University Press: Oxford, U.K., 1990.
- (23) Kukushkin, V. Y.; Pombeiro, A. J. L. *Chem. Rev.* **2002**, *102*, 1771.
- (24) (a) Ma, M.; Stasch, A.; Jones, C. *Chem.—Eur. J.* **2012**, *18*, 10669. (b) Lopez, L. P. H.; Schrock, R. R.; Müller, P. *Organometallics* **2008**, *27*, 3857. (c) Cross, J. L.; Garrett, A. D.; Crane, T. W.; White, P. S.; Templeton, J. L. *Polyhedron* **2004**, *23*, 2831. (d) Tsai, Y. C.; Stephens, F. H.; Meyer, K.; Mendiratta, A.; Gherorghiu, M. D.; Cummins, C. C. *Organometallics* **2003**, *22*, 2902. (e) Young, C. G.; Philipp, C. C.; White, P. S.; Templeton, J. L. *Inorg. Chem.* **1995**, *34*, 6412. (f) Barry, J. T.; Chacon, S. T.; Chisholm, M. H.; Huffman, J. C.;

- Streib, W. E. *J. Am. Chem. Soc.* **1995**, *117*, 1974. (g) Cotton, F. A.; Hall, W. T. *J. Am. Chem. Soc.* **1979**, *101*, 5094. (h) Duchateau, R.; Williams, A. J.; Gambarotta, S.; Chiang, M. Y. *Inorg. Chem.* **1991**, *30*, 4863. (i) Esjornson, D.; Derringer, D. R.; Fanwick, P. E.; Walton, R. A. *Inorg. Chem.* **1989**, *28*, 2821. (j) De Boer, E. J. M.; Teuben, J. H. J. *Organomet. Chem.* **1978**, *153*, 53. (k) Cotton, F. A.; Hall, W. T. *Inorg. Chem.* **1978**, *17*, 3525. (l) Finn, P. A.; King, M. S.; Kilty, P. A.; McCarley, R. E. *J. Am. Chem. Soc.* **1975**, *97*, 220.
- (25) Crystal data for compound **11**: formula = $C_{39}H_{17}BF_4N_2OP_2W_2$, molecular weight 1046.00, monoclinic, space group = $P2_1/n$, $a = 14.724(4)$ Å, $b = 17.519(6)$ Å, $c = 15.276(5)$ Å, $\beta = 104.57(5)^\circ$, $V = 3814(2)$ Å³, $Z = 4$.
- (26) (a) Alvarez, M. A.; García, M. E.; García-Vivó, D.; Ramos, A.; Ruiz, M. A. *Inorg. Chem.* **2011**, *50*, 2064. (b) Alvarez, M. A.; García, M. E.; García-Vivó, D.; Ramos, A.; Ruiz, M. A. *Inorg. Chem.* **2012**, *51*, 11061.
- (27) (a) Riera, V.; Ruiz, M. A.; Villafañe, F.; Bois, C.; Jeannin, Y. *Organometallics* **1993**, *12*, 124. (b) Alvarez, M. A.; García, M. E.; Ramos, A.; Ruiz, M. A. *Organometallics* **2007**, *26*, 1461. (c) Alvarez, M. A.; García, M. E.; Ramos, A.; Ruiz, M. A.; Lanfranchi, M.; Tiripicchio, A. *Organometallics* **2007**, *26*, 5454. (d) García, M. E.; García-Vivó, D.; Ruiz, M. A. *J. Organomet. Chem.* **2010**, *695*, 1592. (e) Alvarez, M. A.; García, M. E.; Menéndez, S.; Ruiz, M. A. *Organometallics* **2011**, *30*, 3694.
- (28) Carty, A. J.; MacLaughlin, S. A.; Nucciarone, D. In *Phosphorus-31 NMR Spectroscopy in Stereochemical Analysis*; Verkade, J. G., Quin, L. D., Eds.; VCH: Deerfield Beach, FL, 1987; Chapter 16.
- (29) Alvarez, M. A.; Anaya, Y.; García, M. E.; Riera, V.; Ruiz, M. A. *Organometallics* **2004**, *23*, 433.
- (30) Yamamoto, Y. *Coord. Chem. Rev.* **1980**, *32*, 193.
- (31) Yamamoto, Y.; Yamazaki, H. *Inorg. Chem.* **1986**, *25*, 3327.
- (32) Fukushima, T.; Kobayashi, K.; Nomura, T.; Tanase, T.; Yamamoto, Y. *Inorg. Chem.* **1994**, *33*, 32.
- (33) Fukushima, T.; Kobayashi, K.; Nomura, T.; Tanase, T.; Yamamoto, Y. *Inorg. Chem.* **1993**, *32*, 4578.
- (34) Martins, A. M.; Calhorda, M. J.; Romao, C. C.; Völk, C.; Kiprof, P.; Filippou, A. C. *J. Organomet. Chem.* **1992**, *423*, 367.
- (35) Filippou, A. C.; Grünleitner, W.; Völk, C.; Kiprof, P. *Angew. Chem., Int. Ed. Engl.* **1991**, *30*, 1167.
- (36) Alt, H. G.; Frister, T. J. *Organomet. Chem.* **1985**, *293*, C7.
- (37) Alvarez, M. A.; García, M. E.; Ruiz, M. A.; Vega, M. F. *Dalton Trans.* **2011**, *40*, 8294.
- (38) (a) Fujita, K.; Nakaguma, H.; Hanasaka, F.; Yamaguchi, R. *Organometallics* **2002**, *21*, 3749. (b) Werner, H.; Zolk, R.; Hofmann, W. J. *Organomet. Chem.* **1986**, *302*, 65. (c) Fischer, H.; Hoffmann, P.; Kreissl, F. R.; Schrock, R. R.; Schubert, U.; Weiss, K. *Carbyne Complexes*; VCH: Weinheim, Germany, 1988. (d) Pombeiro, A. J. L.; Guedes da Silva, M. F. C.; Michelin, R. A. *Coord. Chem. Rev.* **2001**, *218*, 43. (e) Adams, R. D.; Babin, J. E.; Kim, H. S. *Polyhedron* **1988**, *7*, 967.
- (39) (a) Adams, R. D.; Golembesky, N. M. *J. Am. Chem. Soc.* **1979**, *101*, 2579. (b) Prest, D. W.; Mays, M. J.; Raithby, P. R. *J. Chem. Soc., Dalton Trans.* **1982**, 2021. (c) García-Alonso, F. J.; García-Sanz, M.; Riera, V.; Anillo-Abril, A.; Tiripicchio, A.; Ugozzoli, F. *Organometallics* **1992**, *11*, 801. (d) Cabon, N.; Pétillon, F. Y.; Schollhammer, P.; Talarmin, J.; Muir, K. W. *Dalton Trans.* **2004**, 2708.
- (40) Armarego, W. L. F.; Chai, C. *Purification of Laboratory Chemicals*, 5th ed.; Butterworth-Heinemann: Oxford, U.K., 2003.
- (41) Connelly, N. G.; Geiger, W. E. *Chem. Rev.* **1996**, *96*, 877.
- (42) Frisch, M. J. et al. *Gaussian 03, Revision B.02*; Gaussian, Inc.: Wallingford, CT, 2004.
- (43) Becke, A. D. *J. Chem. Phys.* **1993**, *98*, 5648.
- (44) Lee, C.; Yang, W.; Parr, R. G. *Phys. Rev. B* **1988**, *37*, 785.
- (45) Hay, P. J.; Wadt, W. R. *J. Chem. Phys.* **1985**, *82*, 299.
- (46) (a) Hariharan, P. C.; Pople, J. A. *Theor. Chim. Acta* **1973**, *28*, 213. (b) Petersson, G. A.; Al-Laham, M. A. *J. Chem. Phys.* **1991**, *94*, 6081. (c) Petersson, G. A.; Bennett, A.; Tensfeldt, T. G.; Al-Laham, M. A.; Shirley, W. A.; Mantzaris, J. J. *J. Chem. Phys.* **1988**, *89*, 2193.
- (47) Portmann, S.; Lüthi, H. P. MOLEKEL: An Interactive Molecular Graphics Tool. *CHIMIA* **2000**, *54*, 766.
- (48) Ortiz, J. C.; Bo, C. *Xaim*; Departamento de Química Física e Inorgánica, Universidad Rovira i Virgili: Tarragona, Spain, 1998.
- (49) Sheldrick, G. M. *Acta Crystallogr.* **1990**, *A46*, 467.
- (50) Sheldrick, G. M. *Acta Crystallogr.* **2008**, *A64*, 112.